

High duty cycle and continuous terahertz emission from germanium

Erik Bründermann^{a)}

Ruhr-University Bochum, Physical Chemistry II-NC 7/68, D-44780 Bochum, Germany

Danielle R. Chamberlin and Eugene E. Haller

Lawrence Berkeley National Laboratory and University of California, Berkeley, California 94720

(Received 23 February 2000; accepted for publication 28 March 2000)

We measured laser emission from Be-doped Ge crystals with intercontact distances as small as 0.5 mm. An improved heat sink allowed a twofold increase of the laser duty cycle to 5%. We also report the measurements of THz emission from small Be-doped Ge crystals under continuous excitation with volumes as small as 0.5 mm³. © 2000 American Institute of Physics.
[S0003-6951(00)03721-9]

In the far-infrared wavelength or terahertz frequency range (1–10 THz) there are a wide variety of potential applications for compact and tunable lasers. High resolution spectroscopy is relevant to such diverse fields as astronomy, biochemistry, and physical chemistry. Objects of interest include star-forming regions in the universe, heavy ligands in biomolecules which vibrate and rotate with absorption features in the far-infrared, or molecular clusters which give insights into molecular potentials.¹ Any progress in THz laser technology will also have an impact on broad band communication, e.g., intersatellite links.

Ideally a coherent, compact, powerful, tunable, and solid state source is desired. Up to now, the only demonstrated semiconductor lasers in this frequency range are based on bulk *p*-type germanium crystals. We can distinguish two laser mechanisms in Ge. The first mechanism is based on a hole population inversion between the light and heavy hole Landau levels which develops in crossed electric and magnetic fields. The light hole states represent the upper laser states. These lasers are magnetically tunable from 1 to 4 THz.² The second mechanism does not require a magnetic field but is instead based on the splitting of the light and heavy hole band and their respective acceptor states under uniaxial stress. A hole population inversion forms within those acceptor states with the excitation of an electric field at a pressure of more than 3 kbar. The laser emission is tunable by the applied uniaxial stress. Emission frequencies were measured in a pulsed mode from 4.8 to 5.6 THz with a pressure around 7 kbar.³ Recently, continuous wave laser action has been reported for these stressed lasers.⁴ There have been also investigations of Ge lasers in crossed electric and magnetic fields with simultaneous applied uniaxial stress.⁵ It is worth noting that the small Ga-doped Ge lasers in that study did not operate at zero stress but reached high laser duty cycles of around 0.2% if uniaxial stress in excess of 1.3 kbar was applied. Although far-infrared emission from compound semiconductor quantum structures has been detected,⁶ so far no laser emission has been demonstrated. This may be due to the fundamental problem that such devices are small in comparison to the rather large far-infrared wavelength which

leads to a poor coupling between the gain volume and the optical field.

In this letter we present significant progress obtained with high duty cycle, Be-doped Ge lasers in crossed electric and magnetic fields. We also demonstrate THz emission from continuously excited germanium laser material in this configuration. The properties of our samples are given in Table I. The detailed method of the crystal preparation and characterization has been described elsewhere.^{7,8} Wafers were cut from Czochralski-grown crystals with an ID saw. Prior to implantation and metallization, the two opposite sides of the wafer were optically polished to obtain a constant intercontact distance which equals the wafer thickness. Small laser samples were cut from those wafers by using a dicing saw with a blade of 1.5 mm thickness and a diamond grit size of 4–6 μm . Due to the fine grit of the blade and the difficulty to polish such small surfaces no additional mechanical polishing was used. Saw damage was partially removed by a single, 45 s long, chemical etching step using 4:1 HNO₃:HF. The resulting sample surface parallelity was not better than 1 arcmin. The crystal edges are especially vulnerable to saw damage which can result in uneven edges. We expect that surface imperfections lead to a reduced performance, especially for the small samples with dimensions of less than 1 mm used in this study. Edge imperfections are less significant for the larger lasers used in earlier studies.^{7,9}

For laser operation the crystals and the detector were immersed in liquid helium (LHe) at 4.2 K. We used a small superconducting coil to apply a magnetic induction (*B*) up to 3 T for the Faraday configuration.⁷ The available sample space was limited to the 10 mm diameter clearance of the coil. For the Voigt configuration two NdFeB permanent

TABLE I. Tested Ge lasers: Be doping concentration N_A , length *L*, width *b*, contact distance *d*. Crystal orientations along *b* is (110)||**B**, along *d* (001)||**E** also crystal growth direction.

	N_A (10^{20} m^{-3})	$L \times b \times d$ (mm^3)
L0	1.4	$18 \times 3.0 \times 3.0$
L1	1.5	$11 \times 2.5 \times 0.8$
L2	0.16	$0.5 \times 0.5 \times 2.0$
L3	0.3	$1.0 \times 0.5 \times 1.0$
L4	1.5	$20 \times 2.8 \times 0.5$

^{a)}Electronic mail: Erik.Brundermann@ruhr-uni-bochum.de

magnets^{10,11} of size $20 \times 10 \times 10 \text{ mm}^3$ with a remanent magnetization of $B_R = 1.2 \text{ T}$ were placed at opposite sides of the laser crystals separated by a distance of 3 mm which results in a magnetic induction of $B = 0.7 \text{ T}$ across the laser. The multimode laser emission ranges from 70 to 90 cm^{-1} at $B = 0.7 \text{ T}$,² close to the optimum sensitivity of the Al-doped Ge photoconductor at 90 cm^{-1} used in this study.

To improve the heat conduction from the laser to the LHe bath we made a new heat sink using high purity copper (HP Cu) with a Cu purity of 99.999% instead of oxygen free high conductivity (OFHC) Cu with a Cu purity of 99.95% which was used in earlier experiments.⁹ The heat sinks were attached to the ohmic contacts of all lasers with the exception of sample L2. L2 was mounted on a brass holder in the center of a 3 mm circular high quality brass cavity to allow efficient photon collection. The radiation was coupled out through a 1 mm diameter hole. For the other samples no external cavity was used because the high refractive index of Ge allows laser operation using only the crystal surfaces as mirrors for internal reflections. The applied electric field was either pulsed with variable pulse length (0.1–100 μs) and repetition rate (1 Hz–100 kHz) or supplied by a constant high voltage source in the direct-current (dc) mode. The pulse generator circuit was designed to act as a constant voltage source during the pulse. The sample resistance varies by only a few percent during the pulse which results in a similarly shaped, square current pulse. However, the optical pulse has a decay time due to heating,^{9,12} similar to laser pulse shapes obtained previously.⁹ The detected emission was observed on a 500 MHz digital oscilloscope or in the dc mode directly with a multimeter. No amplifier was used.

For the evaluation of the new heat sink we have tested laser L5 from Ref. 9 (identical to L0 in Table I) under the same electrical conditions without any alterations to the crystal. The HP Cu heat sink led to a more than twofold increase in power dissipation, repetition rate, and duty cycle in comparison to the previously used OFHC Cu heat sink. This improvement can be due to a somewhat larger surface area of the new heat sink as well as to the higher heat conduction of the purer Cu material which leads to a larger temperature gradient at the heat sink surface. The limiting mean applied power for L0 was raised from 8 to 17 W. From this result we can assume that the crystal temperature does not exceed 25 K for an applied electrical power of 15 W.⁹

Sample L1 has a small intercontact distance of 0.8 mm which provides faster heat transport from the center plane to the cooled contacts. We have measured the laser emission of L1 up to a duty cycle of $\text{dc} = 5\%$, limited only by our pulse generator. Figure 1 shows the emission intensity at a duty cycle of 5%. At a duty cycle of 1% we measured laser emission up to an electric field of 1.8 kV/cm with the maximum emission at 0.8 kV/cm which is a result of the optical phonon resonance at $E/B = 1 \text{ kV}/(\text{cm T})$.⁷ At a duty cycle of 5% we clearly observe laser emission in the range from 0.4 to 0.65 kV/cm which corresponds to a population inversion induced by resonances with the Be dopant atoms.⁷ We could measure the main peak at 0.8 kV/cm only partially up to 0.7 kV/cm because of power limitations in the pulse generator circuit at such high repetition rates.

We have also tested laser L4 with an intercontact dis-

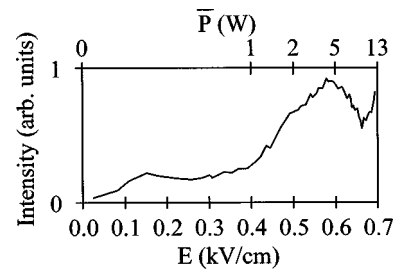


FIG. 1. Laser emission of L1 vs the electric field E at a duty cycle of $\text{dc} = 5\%$ ($t = 10 \mu\text{s}$, $f = 5000 \text{ Hz}$). The mean applied input power is given as $\bar{P} = P \times \text{dc}$. The constant magnetic field was $B = 0.7 \text{ T}$ using permanent magnets.

tance of only 0.5 mm. Laser emission was observed but we could not reach comparable duty cycles of 5%. We speculate that the lower duty cycle is due to imperfections in preparing such small surfaces.

Figure 2 shows far-infrared emission of the lightly doped sample L2 mounted in the brass holder under continuous [$\text{dc} = 1$, Fig. 2(a)] and under pulsed excitation [$\text{dc} \ll 1$, Fig. 2(b)]. The much lower heat dissipation of brass was partially compensated by using a small and lightly doped Ge sample which had a power consumption of about 2–4 W at a voltage of 100 V. The emission of L2 at 0.05 kV/cm (10 V) drops at higher magnetic fields. This is expected because of the current decrease with increasing magnetoresistance. The signal is mainly thermal and follows the input power. At 0.15 kV/cm (30 V), however, we observe a dramatic change in the behavior. The emission first rises and then drops, similar to the typical laser emission behavior of Ge:Be lasers.⁷ Above 0.2 T the curve resembles the curve at 10 V because for $E/B < 0.6 \text{ kV}/(\text{cm T})$ ^{7,13} and at moderate magnetic fields no laser emission is expected (cf. also Fig. 1). Above 0.5 T an increase of emission is observed which can be related to the on-set of cyclotron resonance type emission due to significant splitting of the light hole Landau levels. The absence of such an effect at 10 V suggests that the number of free carriers is too low. At $E = 0.5 \text{ kV/cm}$ (100 V) only a flat curve with minor dependence on the magnetic field is observed which indicates that the sample is far hotter than the heat sink so that the magnetic field cannot freeze out the carriers. At 100 V in a pulsed mode [Fig. 2(b)] we recover the usual laser behavior with typical emission peaks related to various resonances with Be impurities and optical phonons.

Figure 3(a) shows the small, higher doped sample L3

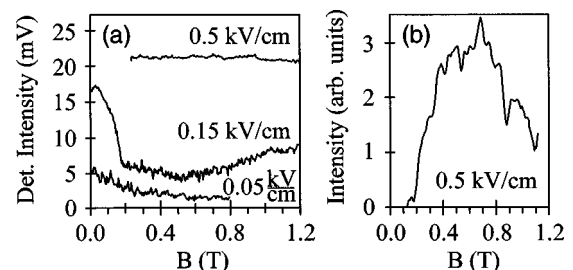


FIG. 2. Far-infrared emission intensity of L2 shown as change in voltage drop across the photoconductor detector vs the magnetic induction B (a) for different constant, continuous ($\text{dc} = 1$) voltages (10, 30, and 100 V) and electric fields E , respectively. (b) for 100 V voltage pulses at a low repetition rate ($t = 10 \mu\text{s}$, $f = 2 \text{ Hz}$). Here we used the superconducting magnet for generating a variable magnetic field.

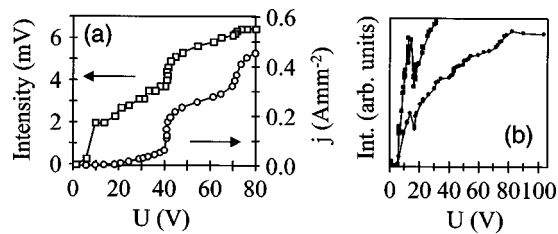


FIG. 3. Far-infrared emission intensity of L3 vs voltage bias. (a) The current density $j=I/(Lb)$ at $dc=1$ and the emission intensity are also shown. The latter is given by the change in voltage drop across the photoconductor detector. (b) Intensity for different detector bias settings and voltage steps. The constant magnetic field was $B=0.7$ T using permanent magnets.

under continuous excitation using the HP Cu heat sinks. There is a clear, nonlinear increase in current density at higher voltages. The first current increase at $E=0.4$ kV/cm results from the on-set of heavy hole scattering with Be impurities. This corresponds, typically, to the on-set of laser action.¹³ The second increase is related to heavy hole scattering with optical phonons and is close to the maximum laser emission of Be-doped Ge lasers at $E/B=1$ kV/(cm T).

We also observe that the intensity curve follows this behavior which can be either thermal or due to transitions of light to heavy hole levels. For a conservative estimate of the thermal component in this emission we have used a maximum temperature of 25 K (input power is 12 W at 70 V) and calculated the expected detector signal of the corresponding blackbody with an optimal detector peak response of 1000 V/W. We also took into account the spectral response of the detector which was measured by a Fourier-transform spectrometer as well as the distance of the detector to the emitting sample of 37 mm and a collection area of 4.4 mm². At 70 V we estimate the contribution of the thermal radiation to the signal to be 3 mV which is half of the observed signal.

Figure 3(b) shows two intensity measurements for different detector bias settings and smaller voltage steps. An indication of nonthermal behavior is found above 80 V where the intensity decreases with increasing input power. A second nonthermal feature is observed between 10 and 20 V (or 0.1–0.2 kV/cm) which resembles a similar peak in the emission of high duty cycle lasers (cf. also Fig. 1). The origin of this peak could be related to cyclotron resonance type transitions between light hole levels which are substantially split at $B=0.7$ T.

In summary, we have demonstrated Ge:Be lasers with small volumes which operate with duty cycles as high as 5% by using an improved heat sink and small intercontact distances. Our current technique to prepare small surfaces seems to lead to imperfections preventing strong laser radiation for samples with a dimension of less than 0.8 mm in one direction. Results under continuous excitation show nonthermal, partially nonlinear signal dependencies which may be related to optical gain. With a more precise surface preparation a strong continuous wave laser in the far-infrared wavelength and THz frequency range appears to be in reach. Further optimization of the heat sink geometry is possible, e.g., by using multiple fins.

One experimental problem is the high LHe consumption due to the power input of about 10 W. This leads to a He gas flow of 3 l per second which prohibits long duration experiments such as spectral measurements due to substantial freezing of the venting system. However, closed-cycle refrigerators can be used to operate Ge lasers¹¹ and commercially available machines can cool down to 10 K at 10 W without any freezing problems. The cube-like sample geometry used in our experiments was dictated by the current fabrication process and is also far from optimal due to the strong inhomogeneity of the electric field. Our recently demonstrated planar structure¹⁴ in combination with a thin doped active layer has the potential of combining a homogeneous electric field distribution and a relatively large sample size due to the integrated Ge heat sink. The latter simplifies mechanical optical polishing. With an optimized laser resonator we expect that we can realize a reduced active volume and doping concentration to allow strong continuous wave laser operation at moderate input powers.

This work was supported by the Director, Office of Science, Office of Basic Energy Sciences, Division of Materials Sciences of the U.S. Department of Energy under Contract No. DE-AC03-76SF00098. One of the authors (E.B.) acknowledges support by the Alexander-von-Humboldt Foundation through a Feodor-Lynen Fellowship and support by the Center for Particle Astrophysics at UC Berkeley. E.B. also thanks H. P. Röser, DLR Berlin, for the challenge to obtain cw emission from Ge lasers. The authors also thank B. Tang for assistance with wafer polishing. D.R.C. acknowledges the NASA Office of Space Science Fellowship No. S99-GSRP-070 for their support.

- ¹H. Linnartz, W. L. Meerts, and M. Havenith, *Chem. Phys.* **193**, 327 (1995).
- ²L. A. Reichertz, O. D. Dubon, G. Sirmain, E. Bründermann, W. L. Hansen, D. R. Chamberlin, A. M. Linhart, H. P. Röser, and E. E. Haller, *Phys. Rev. B* **56**, 12069 (1997).
- ³I. V. Altukhov, E. G. Chirkova, M. S. Kagan, K. A. Korolev, V. P. Sinis, and I. N. Yassievich, *Phys. Status Solidi B* **198**, 35 (1996).
- ⁴Yu. P. Gousev, I. V. Altukhov, K. A. Korolev, V. P. Sinis, M. S. Kagan, E. E. Haller, M. A. Odnoblyudov, I. N. Yassievich, and K.-A. Chao, *Appl. Phys. Lett.* **75**, 757 (1999).
- ⁵N. Hiromoto, I. Hosako, and M. Fujiwara, *Appl. Phys. Lett.* **74**, 3432 (1999).
- ⁶M. Rochat, J. Faist, M. Beck, U. Oesterle, and M. Illegems, *Appl. Phys. Lett.* **73**, 3724 (1998).
- ⁷E. Bründermann, A. M. Linhart, L. A. Reichertz, H. P. Röser, O. D. Dubon, G. Sirmain, W. L. Hansen, and E. E. Haller, *Appl. Phys. Lett.* **68**, 3075 (1996).
- ⁸E. E. Haller and E. Bründermann, US Patent No. 6,011,810 (4 January 2000).
- ⁹E. Bründermann, D. R. Chamberlin, and E. E. Haller, *Appl. Phys. Lett.* **73**, 2757 (1998).
- ¹⁰K. Park, R. E. Peale, H. Weidner, and J. J. Kim, *IEEE J. Quantum Electron.* **32**, 1203 (1996).
- ¹¹E. Bründermann and H. P. Röser, *Infrared Phys. Technol.* **38**, 201 (1997).
- ¹²P. D. Coleman and D. W. Cronin, *Int. J. Infrared Millim. Waves* **18**, 1241 (1997).
- ¹³E. Bründermann, D. R. Chamberlin, and E. E. Haller, *Infrared Phys. Technol.* **40**, 141 (1999).
- ¹⁴D. R. Chamberlin, E. Bründermann, and E. E. Haller, *Appl. Phys. Lett.* **74**, 3761 (1999).